Stockholm University
Department of Astronomy

Bachelor of Science Thesis

Population III and Dark Stars at High Redshifts

Counting stars in the field of view of the James Webb Space Telescope

by

Claes-Erik Rydberg

Supervisor: Erik Zackrisson

Stockholm, february 2009

Abstract

A lot of work has been done on population III stars, which are supposed to provide the first enrichment of the heavier elements observed in the universe. Dark stars are a special class of population III stars powered by dark matter. The James Webb telescope is slated for launch in 2014 and a natural question is whether we will observe any population III stars with it and if so, how many. Here, I derive a formula for calculating the number of stars in the field of view of a telescope as a function of redshift. I then use a model for the star formation rate for population III stars to calculate how many will appear in the field of view of the James Webb telescope under different assumptions. I also do a comparison of my formula to a formula for calculating the number of supernovas observed to show that they in a certain limiting case are equivalent. Finally I calculate the AB-magnitudes of the most luminous population III stars and what magnification from gravitational lensing one would need to observe them.

To Alexandra

Contents

Acknowledgements

First, of course, I would like to thank my supervisor, Erik Zackrisson, for the opportunity to do a very interesting Bachelor of Science thesis. He has helped me both with ideas and comments on the report.

I also would like to thank Michele Trenti for providing me with star formation rate data from his and Stiavelli's simulations. He has also kindly answered my questions and provided explanations when needed.

Thanks also to Fabio Iocco who let me use figure 3.1 from their papers [5] and [6].

Finally I would like to thank my girlfriend Alexandra for her support and helpful comments on the design of the report.

Introduction

This thesis is the final part in my Bachelor of Science education at the department of astronomy at Stockholm university. It is a work in cosmology regarding the first stars in the universe. It was supervised by Erik Zackrisson in the galaxy and cosmology group.

The thesis is split into seven chapters, each covering a logically related part of the thesis. There are also three appendices with material that is not necessary for the main results but can clarify and explain parts of it. One appendix is a printout of the main part of the code used for the calculations in the thesis. Below follows a listing with a very short explanation and motivation of each chapter in the thesis.

1 **The Big Bang** This chapter gives some background information about the Big Bang and the different phases the universe has evolved through. This is to stress the importance of the unknown phase where population III stars and dark stars are postulated to exist.

2 **Population III stars** This is an overview of population III stars, their formation and possible detection. A brief explanation of the models for star formation used in this thesis is also given.

3 **Dark Stars** This chapter gives an explanation of what dark stars are. It also gives an explanation of the dark matter candidate that is supposed to fuel these objects.

4 **James Webb Telescope** The James Webb Telescope, its instruments and its position in space is summarized.

5 **High Redshift Stars in the Field of View** In this chapter, the main results of the thesis are presented. An equation for calculating the number of stars in the field of view of the James Webb Telescope is derived. This equation is then used to calculate the number of population III stars or dark stars when using the star formation rate models of Trenti & Stiavelli.

6 Gravitational Lensing This is a short explanation of what gravitational lensing is and how it can help us detect stars at high redshift.

7 Conclusions This is a rather speculative field. I nevertheless try to draw some conclusions in this chapter.

Appendices There are three appendices in this thesis. In the first, I present a connection between the formula I derived in this thesis and a formula used for estimating the rate of supernovas observed. In the second, I explain some measures of distances used in cosmology and how they connect to the formula derived in the thesis. The last appendix is a printout of the main code used for calculating the results in this thesis.

Chapter 1

The Big Bang

How did the universe start? Galaxies recede faster the farther away they are, the cosmic microwave background and the fact that the night sky is black all indicate it all started with an explosion. Our current models point to an origin about 13.7 billion years ago. This is also supported by the fact that no stars older than this have been found.

1.1 Evolution of the Universe

This is a short overview of the evolution of the universe. The idea is to give the reader an understanding of the necessity of a process for forming the heavier elements seen in the observable universe.

1.1.1 Neutrons Form

In the early and very hot universe the newly formed quarks reacted and formed baryonic matter, mainly protons and neutrons. The reaction process between protons and neutrons were in equilibrium but tilted towards neutrons when the universe got colder. This process stopped when the neutrinos which are necessary for the reaction decoupled and stopped interacting with matter. This was a consequence of the universe becoming sufficiently cold. The neutron/proton ratio was then "frozen". This process lasted only about a second.

1.1.2 Nucleosynthesis

Neutrons decay on a rather short timescale, so if nothing interfered, all matter would have become protons. However the protons reacted with neutrons to form heavier elements. This process was so inefficient though that almost only helium and no heavier elements formed. When calculating the ratio of helium with the "frozen" neutron/proton ratio, a helium fraction of 0.24 in the universe results. The rest is hydrogen with some trace amounts of heavier elements, mainly lithium. This process lasted about ten minutes.

1.1.3 Nucleosynthesis to Last Scattering

This period lasts from ten minutes after the Big Bang until 350,000 years after the Big Bang. During this time, the universe goes from a radiation dominated universe to a matter dominated universe (because the energy density for radiation decays faster than the energy density for matter). Recombination also occurs, which means that electrons and hydrogen/helium cores react to form neutral atoms. This poses a conundrum since the universe we observe today is ionized. Hence, at some time after recombination the universe has become ionized again. At the end of this period, photons decouple from matter and the universe becomes transparent. This is closely related to the last scattering, which means the photons that we see from this era in the form of CMB.

1.1.4 Population III Stars / Dark Stars era

This period lasts from 350,000 years after the Big Bang until approximately 480 million years after the Big Bang. It is the era that is examined in this report. The problem that leads to the postulation of population III stars is as follows:

The heavier elements that we can thank for our existence are formed by fusion in the center of stars. This leads to an increase of heavier elements the older the universe becomes (on average). When observing far away there is a gap of the metallicity (heavier elements than helium) between the observations of stars and matter and the almost non-metallicity of the Big Bang. The favoured explanation for this is that there were a class of stars before our farthest observations that produced the heavier elements. These stars are called population III stars and is the subject of section 2.

Dark stars are postulated by the possibility that some candidates for the mysterious dark matter, that hold our galaxies, galaxy groups and galaxy clusters together, are self annihilating. This could power the energy generation of stars instead of the normal fusion. These stars are the subject of section 3.

1.1.5 Population I Stars / Population II Stars era

During this period, the universe is matter dominated and the stars are mainly population II stars and population I stars. The transition from population III stars to population II/population I stars is probably prolonged. They could very well live at the same time in different parts of the universe. This is the era we are living in.

Chapter 2

Population III stars

As mentioned in 1.1.4 population III stars are postulated to exist between the time of the Last scattering (CMB) and the farthest observed objects in the universe. This is because the universe has to be enriched with metals, compared to what was created in the Big Bang. In the so called recombination,* the electrons and atom nuclei combined to form neutral atoms. The present-day universe is ionized so a reionization must have taken place. Population III stars are likely to have contributed to this.

2.1 Formation

There has been a wealth of research on the formation of population III stars. The general results is that they were probably very massive, weighing in at approximately 100 $M_\odot$ with a span of 60 $M_\odot$ to 300 $M_\odot$. They were also short lived, typically 2 million years. The likely formation sites are in dark matter halos where normal matter accumulated. As described in [1], probably only one star per halo could be created. This follows as the massive star that is formed emits a lot of UV radiation which destroys the H_2 in the parent cloud that is necessary for future cooling during formation. Simulations [16] of protostar formation have confirmed the average mass of population III stars as $\sim$100 $M_\odot$.

2.2 Star Formation Rate Models

Trenti and Stiavelli [15] have done extensive modeling of the star formation rate for population III stars. It is built on Press-Schechter modeling coupled with analytic recipes for gas cooling and radiative feedback. In their paper, they have

*This should really be called the Combination since there was no earlier combination.

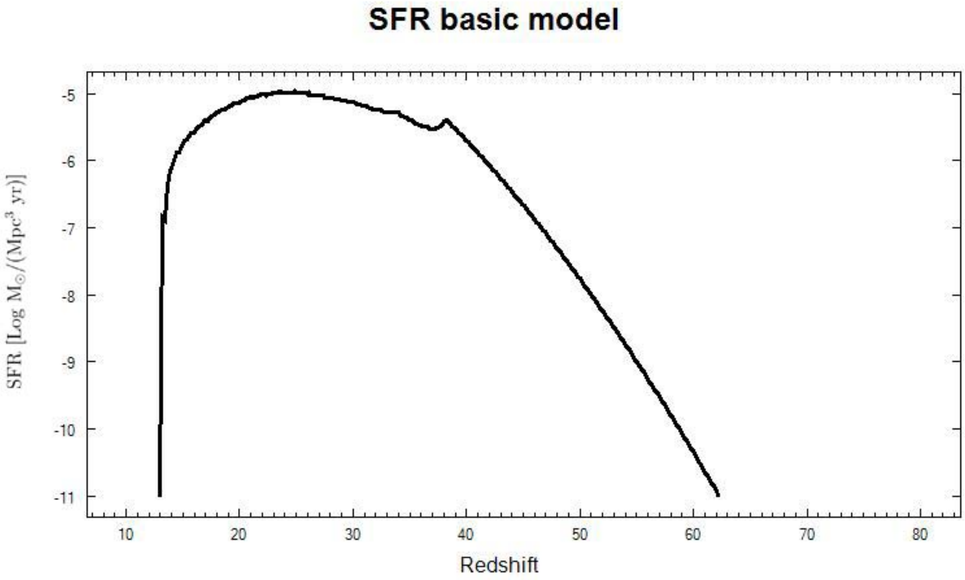

Figure 2.1: SFR in Basic model

implemented 8 different models based on different assumptions. We will use the three first, as they are most interesting for our dark star approach. The three models are described below. Model 2 and 3 are especially interesting for dark star calculations, as dark stars are likely to be cooler than population III stars and thus emit less radiation in the LW band. Most of the calculations in this report will build on those three models. Please note that the models we use form stars with H_2 cooling. There might be formation of population III stars at lower redshift in halos with $T_{vir} > 10^4$. The H_2 cooling models have been chosen because these are most interesting for the possible formation of dark stars. Dark stars are most probably formed as single stars in halos where H_2 cooling dominates star formation.

2.2.1 Model 1: Basic Model

The basic model produces at most one star per dark matter halo. The star has an average mass of 100 $M_\odot$ with a Salpeter distribution in the span 50 $M_\odot$ to 300 $M_\odot$. Half of the photons in the LW band escape which dissociates H_2, thereby temporarily suppressing further star formation. The resulting star formation rate as a function of z can be seen in figure 2.1.

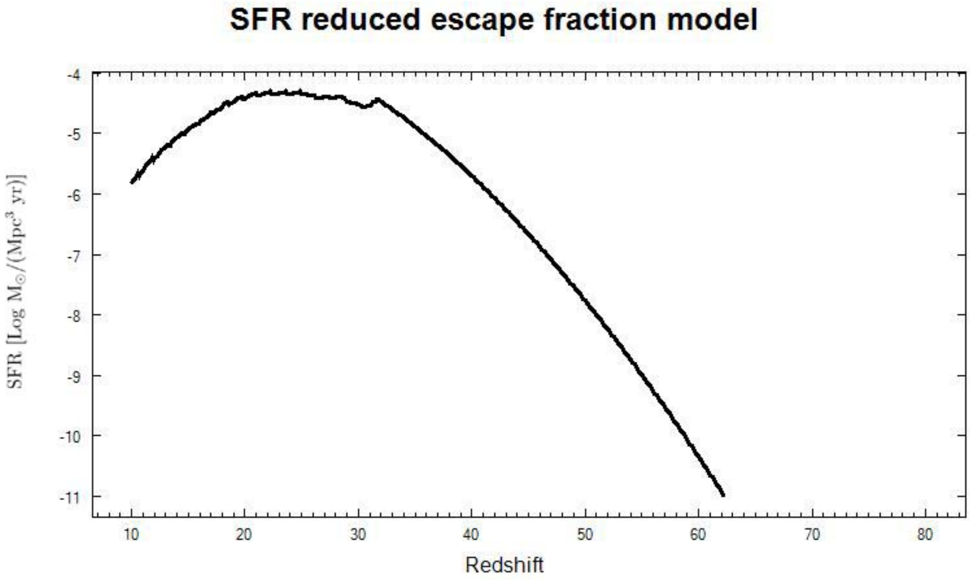

Figure 2.2: SFR in Reduced escape fraction model

2.2.2 Model 2: Reduced Escape Fraction

This model differs from the first model in that the fraction of photons in the LW band that escape is reduced by a factor 10. This leads to a higher star formation rate which also lasts longer, as can be seen in figure 2.2. The calculation is stopped at z=10 because the analytical model for metal enrichment only takes into account self-enrichment and not wind enrichment, which becomes important at this redshift.

2.2.3 Model 3: No Lyman-Werner Feedback

This model is like model 2, except that the LW feedback fraction is set to zero. This increases the star formation rate even more and prolongs it. The result can be seen in figure 2.3.

2.3 Detection

Even though mostly theoretically postulated, there are some detection candidates for population III stars. In [3] one possible candidate is mentioned in a lensed dwarf galaxy at z=3.4. A galaxy at z=6.5 is also mentioned as a candidate. If the Trenti and Stiavelli models hold, those redshifts are probably too low to hold population III stars formed through H_2 cooling. Of course, either the models

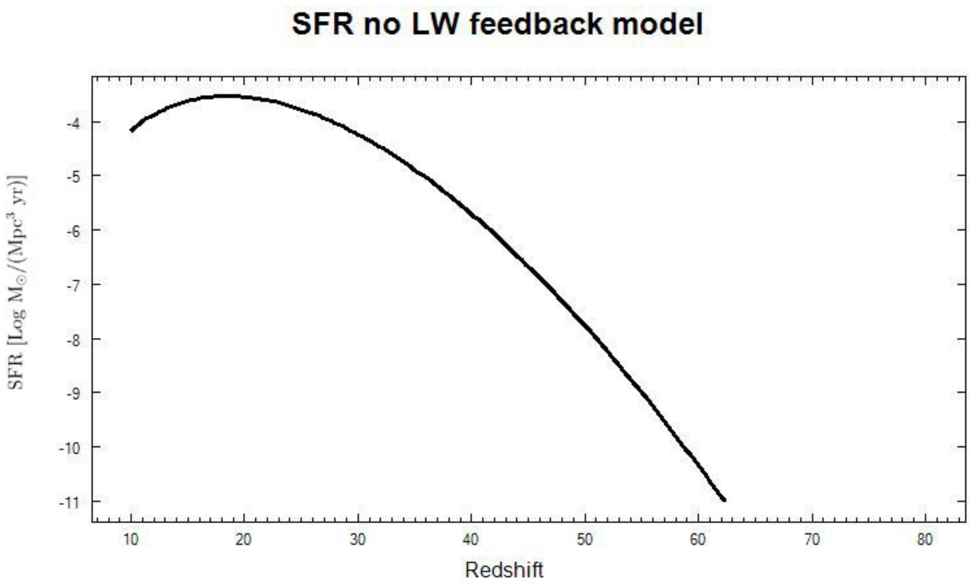

Figure 2.3: SFR No Lyman-Werner feedback model

could not be true or they could be formed in $T_{vir} > 10^4$ K halos, given that those form population III stars at those redshifts.

The Cosmic Infrared Background radiation is a repository of emission of radiation through the entire universe. It contains radiation that was emitted at other wavelengths but has been redshifted into the infrared. Kashlinsky, [7], shows the possibility that we see the fingerprints of population III stars in the measurement of the CIB. Through this method, an indirect detection of population III stars might already have been achieved.

Chapter 3

Dark Stars

Dark stars represent a special kind of population III stars. Their energy comes from self annihilating dark matter particles.

3.1 Dark Matter

When measuring the speed of rotation for stars in a spiral galaxy, the speed as a function of the radius is expected to be decreasing. On the contrary, the rotational velocity typically assumes a constant value outside the core of the galaxy. The most common way to solve this is to postulate that there is more matter in the galaxy that we can not see, the so called dark matter. Similarly, it can be shown that galaxies in galaxy clusters have too high velocities to be gravitationally bound, if the calculations are based only on the matter we can see directly.

Weakly Interacting Massive Particles (WIMP:s) that are their own anti particles represent a popular candidate for dark matter. Particles that are their own anti particles self annihilate upon collision, releasing energy. Those particles also produce roughly the correct abundance to account for the observed dark matter, the so called WIMP miracle, see [13]. This kind of particle is very interesting for this thesis as it possibly provides the fuel for dark stars.

3.2 Dark Matter Powered Stars

As already mentioned, these are stars where the production of energy comes from self-annihilating dark matter. Dark stars can also be viewed as an evolutionary stage in the life of population III stars, as the protostar evolution towards the main sequence is halted when powered by dark matter. The effects have been studied in [5], [6] among others, and the results can be seen in figure 3.1, which

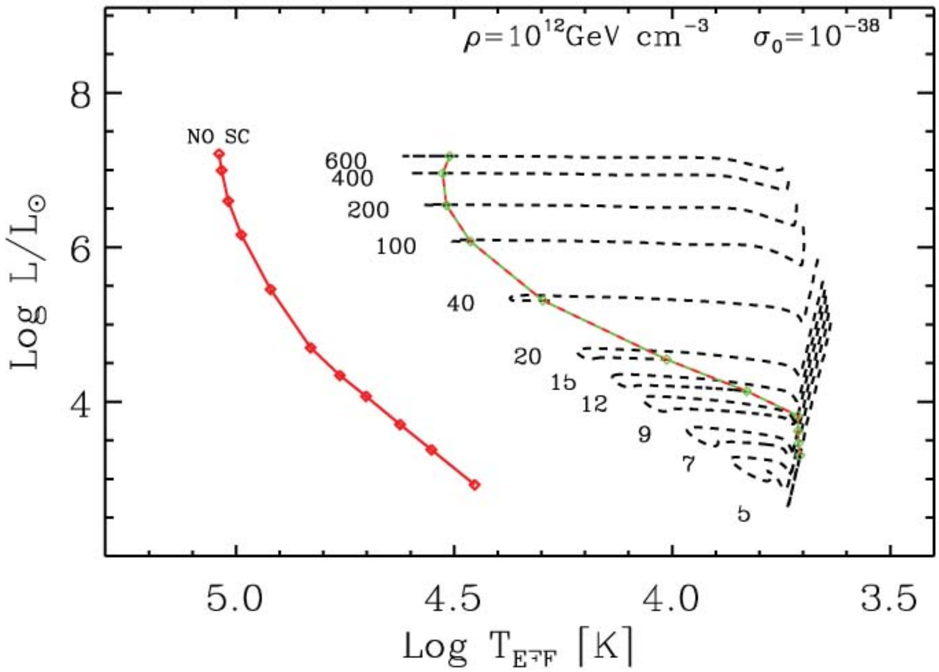

Figure 3.1: HR diagram for metal-free stars in presence of a DM environmental density $\rho = 10^{12}$ GeV and the elastic scattering cross section between WIMP and baryons $\sigma = 10^{-38}$, compared to their normal position in the HR; solid curve labeled NO SC. For all masses, the ZAMS is never reached, as stars are entirely supported by DM annihilation.

is reproduced from their article. As can be seen the evolution of the stars is halted and they become dark stars for a period of time which depends on the abundance and properties of dark matter. When the dark matter in the star is depleted because of annihilation, the star continues its evolution and becomes a normal population III star. The time spent as dark star can possibly be prolonged by scattering of dark matter. Dark matter from the halo still surrounding the star scatters against baryonic matter until it ends up in the star and annihilates. This process depends a lot on the scattering cross section between dark matter and baryons.

In [14], Freese et al. model the evolution of the dark star stage with polytropic models of the interior of the star and model the accretion of matter from the surrounding volume. They end up with cool (T_{eff} <10,000 K), large (R=1−10 AU), bright ($L=10^6 - 10^7$ $L_\odot$) and massive (M=500−1000 $M_\odot$) stars. This dark star stage lasts a rather short time, about 400,000 years, but this could be prolonged by scattering, as mentioned above. Of course polytropic models are rather approximative, but they claim that a more thorough calculation at one of the polytropic indices used gives approximatively the same answer. The results are also weakly depending on the uncertainties, such as dark matter particle mass, accretion rate and scattering, always giving cool, massive and large stars.

Chapter 4

James Webb Telescope

Originally known as the "Next Generation Space Telescope", it was renamed in 2002 to the "James Webb Telescope", or JWST for short. It will be a large (6.5 m mirror) infrared telescope which is slated for launch in 2014. It will probably be the premiere observatory of the next decade and beyond. The James Webb Telescope is an international collaboration between NASA, ESA and CSA.

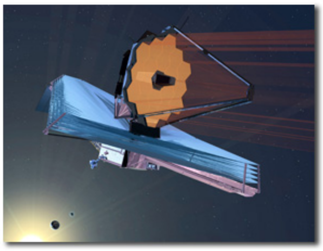

4.1 Hubble Space Telescope

The Hubble Space Telescope was launched in 1990
and placed in orbit around earth, above the atmosphere that blocks part and distorts our view of the universe. The start was a disaster, as the mirror was found to be forged in a slightly wrong shape and the images were distorted. This was fixed with a service mission, and since then, the Hubble Space Telescope has provided us with outstanding science and breathtaking images.

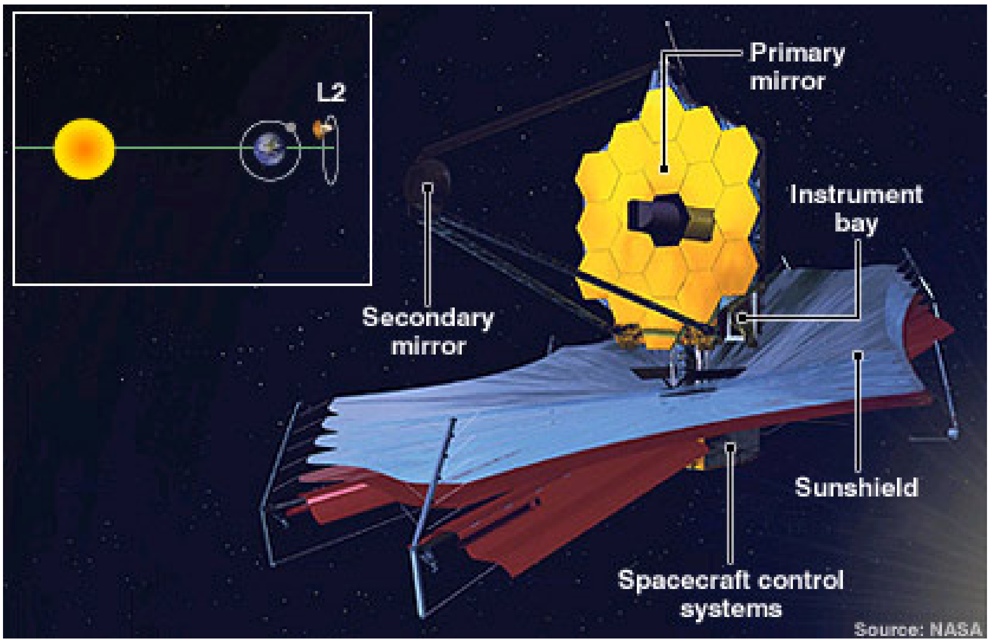

Figure 4.1: JWST close view

4.2 The Successor

As astronomers see more, their appetite is wetted and they just want to see more and have larger mirrors/lenses to collect more light. This is known as aperture fever among amateur astronomers. As a result, a successor to Hubble, the James Webb Telescope is being constructed. It will boast a 6.5 meter primary mirror and will probably see the first galaxies. It will have a sunshield the size of a tennis court.

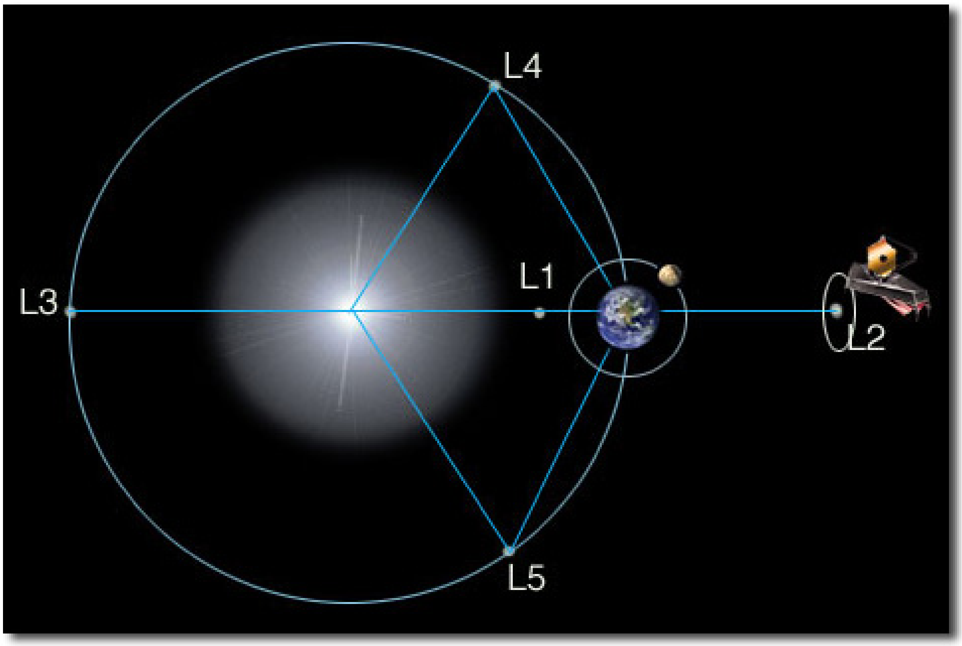

Figure 4.2: JWST position in space

4.3 Lagrange point L2

In the 18th century, the mathematician Joseph-Louis Lagrange found five stable solutions to the three body system. These solutions concern two massive objects, where one of them preferably is much more massive than the other, and one object of negligible mass compared to the other two. Then there are five points at which the small object can be and stay in position relative to the other objects, the so called Lagrangian points L1-L5. Two of them are stable, L4 and L5, meaning that the object stays in position for small perturbations. The other are not stable towards small perturbations and compensation (such as rocket thrusts in the right direction) is necessary.

In our case, the most massive object is the sun, the other massive object the earth and the small object the JWST. A schematic illustration of the situation is presented in figure 4.2. The JWST will be at Lagrangian point L2. This is because the sun, earth and moon could heat up the telescope, which has to be very cold to observe in infrared. At L2 all of these objects are located in the same direction and can be shielded from the telescope with the sunshield. The disadvantage is of course that L2 is unstable, so a rocket thrust will sometimes be necessary to keep the telescope fixed at this point.

4.4 Instruments

The JWST will house four main instruments.

4.4.1 Mid-Infrared Instrument

The MIRI is an instrument that demands a very cold temperature to operate properly, 7 K. To achieve this, there is a pair of cooling systems installed. The instrument will observe in the wavelength interval 5 to 27 micrometers (50,000-270,000 Å). It provides coronography, imaging and low and high resolution spectroscopy. The imaging module will use 1,024 × 1,024 pixels. The maximum field of view will be 1.25 × 1.88 arcminutes.

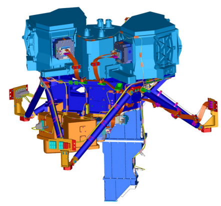

Figure 4.3: MIRI

4.4.2 Near-Infrared Camera

The NIRCam has a wide field of view. It has CCD -like cameras installed to take pictures. It covers a short wavelength of 0.6 to 2.3 micrometers (6,000-23,000 Å) and a long wavelength of 2.4 to 5 micrometers (24,000-50,000 Å) which are used simultaneously. NIRCam has a field of view of 2.2 × 2.2 arcminutes. It has ten mercury-cadmium-telluride (HgCdTe) detector arrays which are analogous to CCDs found in ordinary digital cameras. The short wavelength has a pixel format of 4,096 × 4,096 and the long wavelength has a pixel format of 20,482 × 20,482.

Figure 4.4: NIRCam

4.4.3 Near-Infrared Spectrograph

The NIRSpec will be able to obtain simultaneous spectra of 100 objects or more. This in a 9-square-arcminute field of view. This is accomplished through microshutters that can close the view for a certain cell individually. The microshutters are arranged in a grid containing more than 62,000 shutters. It can provide medium-resolution spectroscopy over a wavelength range of 1 to 5 micrometers (10,000-50,000 Å). Lower-resolution spectroscopy can be achieved for 0.6 to 5 micrometers (6,000-50,000 Å).

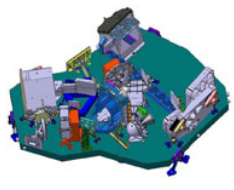

Figure 4.5: NIRSpec

4.4.4 Fine Guidance Sensor

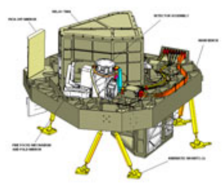

Figure 4.6: FGS

The FGS is used to acquire "guide stars" when observing in a certain direction. It can do that with 95 % probability in any given direction. It also features a wide-field, narrow-band camera that operates between 1.6 and 2.6 micrometers (16,000-26,000 Å) and between 3.1 and 4.9 micrometers (31,000-49,000 Å). The camera can view two adjacent field of views, each of 2.4 × 2.4 arcminutes. This is used to provide support for the ACS, which enables stable pointing at the milli-arcsecond level. There is also a scientific dedicated camera attached to the FGS. This camera has a field of view of 2.2 × 2.2 arcminutes and operates between 1.5 and 5 micrometers (15,000-50,000 Å).

Chapter 5

High Redshift Stars in the Field of View

The objective of this section is to calculate the number of population III or dark stars in the field of view of the JWST. The star formation rate will be based on the models of Trenti & Stiavelli [15] which were described in section 2.2. The results will be integrated through redshifts to get a total number of stars in the field of view of JWST.

5.1 Equation

The equation we will be using integrates through redshifts to get a total number of stars in the field of view. The derivation of this equation is found in section 5.2 and a comparison to a similar equation for supernova observations can be found in appendix A. The models form stars between redshift 10 and 80, but some margin must be included on the low redshift limit. Some stars are formed at this time but live longer, and thus will be observed later than this redshift.

$$N = \int_{z_l}^{z_h} \int_{t(z)}^{t(z)-\tau} SFR(t)dt/M \frac{dt}{dz} c\theta_1\theta_2 d_A(z)^2(1+z)^3 dz \tag{5.1}$$

Different lifetimes of the star will be used. 100 $M_\odot$ will be used as mass for the stars. For θ_1 and θ_2 2.2 arcminutes will be used, as this is the field of view of the NIRCam instrument. As SFR(t) the correct model SFR 2.2 are used. The rest of the values are calculated assuming a flat ΛCDM cosmology with parameters Ω_Λ=0.726, Ω_M=0.274 and H_0=70.5 km s^{-1} Mpc^{-1}, values from [9]. Please note that equation 5.1 does not estimate the number of population III/dark stars sufficiently bright to be observed, but simply the total number within the JWST

Symbol	Description
N	Number of stars in field of view
z_l	Lower limit of redshift
z_h	Higher limit of redshift
t(z)	Cosmic time at redshift z
τ	Life time of star
SFR(t)	Star formation rate at time t
M	Mass of star
$\frac{dt}{dz}$	Time derivative with respect to redshift
c	Speed of light
θ_1	Angular resolution of instrument in horizontal direction
θ_2	Angular resolution of instrument in vertical direction
$d_A(z)$	Angular size distance at redshift z

Table 5.1: Parameters for Stars in Field of View Equation

field of view. Since we will only look at models of star formation using H_2 cooling, there might be stars formed with other types of cooling as well.

5.2 Derivation

The models of Trenti & Stiavelli [15] produce a star formation rate at cosmological time t in $M_\odot$ per comoving Mpc^3 and year. This is SFR(t). By integrating this over an assumed life time of a star and dividing by an assumed stellar mass, we get a number of stars per Mpc^3 at a certain cosmic time.

$$n_t(t) = \int_{t-\tau}^{t} SFR(t)dt/M \tag{5.2}$$

Here, $n_t(t)$ is the resulting number of stars per Mpc^3 at cosmic time t. τ is the life time and M the mass of the stars.

For a small element of our view we can get the proper distance through $d_p = \frac{c}{a(t)}dt$ which is multiplied by $n_t(t)$ to get the number of stars per Mpc^2 of observed area for this interval. This is then transformed to redshift.

$$n_t(t)\frac{c}{a(t)}dt = n_t(t)\frac{dt}{dz}c(1+z)dz \tag{5.3}$$

The area observed at each redshift is deduced with the help of the angular size distance $d_A(z)$. The angular width of the telescope θ_1 and the angular height θ_2, each multiplied with the angular distance and multiplied together, gives the observed area at a certain redshift. Since this is not in co-moving coordinates, we multiply by $(1+z)^2$ to convert it to an area in co-moving coordinates.

$$A(z) = \theta_1\theta_2 d_A(z)^2(1+z)^2 \tag{5.4}$$

By inserting equation 5.2 into equation 5.3 and multiplying with equation 5.4, we get an expression for the number of stars within the field of view in a redshift slice dz:

$$\theta_1\theta_2 d_A(z)^2(1+z)^2\int_{t-\tau}^{t} SFR(t)dt/M\frac{dt}{dz}c(1+z)dz \tag{5.5}$$

This is then integrated between z_l and z_h which is the interval in which we want to calculate the number of observed stars. t(z), which is the cosmic time at redshift z, is inserted instead of t. Equation 5.3 implies integration from z_h to z_l but this is switched as well as the integration order of the inner integral, so the effect of the integration order switch cancels out. We end up with:

$$N=\int_{z_l}^{z_h}\int_{t(z)}^{t(z)-\tau} SFR(t)dt/M\frac{dt}{dz}c\theta_1\theta_2 d_A(z)^2(1+z)^3dz \tag{5.6}$$

Appendix B explains the different cosmic distances and their relations. The relation to these formulas is that the equation 5.2 part of equation 5.6 is evaluated along the life lines of the stars with t(z) equal the cosmic time where the life line crosses the angular size distance. For a redshift slice dz at this crossing is the volume part of equation 5.6. When integrating over z, all of these volumes between z_l and z_h are multiplied by stars formed along similar life lines and summed to the final result equation 5.6.

5.3 Results

To get the number of stars, equation 5.1 is integrated in different redshift bins from 5 to 20. Each bin is integrated with 10 equally sized intervals. The results are shown in tables 5.2, 5.3 and 5.4 corresponding to the three different SFR(t) models we are using. Please note that model 2 and 3 have their SFR cut at redshift 10, so there probably would be some more stars at lower redshift for those models.

For an estimate of the number of population III stars in the field of view, one should probably look at table 5.2 (basic model) for life time 2 million years. The average life time for a population III star is hard to know, but looking at [12] a life time of 2 million years are chosen as a proxy. For an estimate of the number of dark stars in the field of view one should probably look at table 5.3 (reduced escape fraction model) for life time 10 million years. This life time is also a proxy, assuming an extended life time because of dark matter scattering.

In figure 5.1 is a plot of the number of stars in field of view at a redshift below 20. The term Large short lived DS denotes the large, heavy dark stars found in the polytropic models described in section 3.2. The reduced escape fraction model, a star mass of 1000 $M_\odot$ and a life time of 400,000 years has been used for the calculation. Population III stars uses the basic model with life time

	Star lifetime					
Redshift	10^5	10^6	2×10^6	10^7	10^8	5×10^8
5	0	0	0	0	0	0
6	0	0	0	0	0	0
7	0	0	0	0	0	7600
8	0	0	0	0	0	7.2×10^4
9	0	0	0	0	0	1.2×10^5
10	0	0	0	0	0	1.2×10^5
11	0	0	0	0	230	1.1×10^5
12	0	0	0	0	3300	9.8×10^4
13	0.36	3.8	8.1	70	9700	9.1×10^4
14	4.9	50	100	590	1.8×10^4	8.3×10^4
15	9.9	100	200	1100	2.6×10^4	7.6×10^4
16	15	150	300	1600	3.3×10^4	6.8×10^4
17	19	200	390	2100	3.8×10^4	6.0×10^4
18	24	250	490	2600	4.0×10^4	5.3×10^4
19	28	280	570	3000	3.9×10^4	4.6×10^4
20	31	320	630	3300	3.6×10^4	3.9×10^4

Table 5.2: Result, basic model

2 million years. Dark stars, finally, uses the reduced escape fraction model with life time 10 million years. Figure 5.2 plots the same, only extended to redshift 80.

The tables implies that the dark stars have to have a very long life time to be present at lower redshifts. At least if the models for star formation used in this report are true. Model 2 and model 3 probably has star formation at z<10, but it is hard to speculate for how long they will continue. According to the graphs, the redshift where the number of stars peak are at redshift slightly higher than 20.

	Star lifetime					
Redshift	10^5	10^6	2×10^6	10^7	10^8	5×10^8
5	0	0	0	0	0	0
6	0	0	0	0	0	1.2×10^4
7	0	0	0	0	0	1.2×10^5
8	0	0	0	0	0	4.5×10^5
9	0	0	0	0	4600	6.7×10^5
10	7.5	76	150	890	2.0×10^4	6.2×10^5
11	20	200	400	2100	3.3×10^4	5.6×10^5
12	29	290	580	3000	5.0×10^4	5.0×10^5
13	40	400	800	4200	7.3×10^4	4.5×10^5
14	53	530	1100	5500	1.0×10^5	4.0×10^5
15	66	670	1300	7100	1.4×10^5	3.6×10^5
16	83	840	1700	8900	1.7×10^5	3.2×10^5
17	110	1100	2100	1.1×10^4	1.9×10^5	2.8×10^5
18	130	1300	2700	1.4×10^4	1.9×10^5	2.4×10^5
19	150	1500	3100	1.6×10^4	1.8×10^5	2.1×10^5
20	170	1700	3400	1.7×10^4	1.7×10^5	1.7×10^5

Table 5.3: Result, reduced escape fraction model

	Star lifetime					
Redshift	10^5	10^6	2×10^6	10^7	10^8	5×10^8
5	0	0	0	0	0	0
6	0	0	0	0	0	4.7×10^5
7	0	0	0	0	0	3.3×10^6
8	0	0	0	0	0	6.3×10^6
9	0	0	0	0	1.9×10^5	6.7×10^6
10	320	3200	6400	3.7×10^4	7.7×10^5	6.0×10^6
11	780	7800	1.6×10^4	8.1×10^4	1.1×10^6	5.2×10^6
12	970	9800	2.0×10^4	1.0×10^5	1.3×10^6	4.4×10^6
13	1100	1.1×10^4	2.3×10^4	1.2×10^5	1.5×10^6	3.6×10^6
14	1300	1.3×10^4	2.6×10^4	1.3×10^5	1.6×10^6	3.0×10^6
15	1400	1.4×10^4	2.8×10^4	1.4×10^5	1.6×10^6	2.4×10^6
16	1400	1.4×10^4	2.9×10^4	1.5×10^5	1.5×10^6	1.9×10^6
17	1400	1.4×10^4	2.9×10^4	1.5×10^5	1.3×10^6	1.5×10^6
18	1400	1.4×10^4	2.8×10^4	1.4×10^5	1.1×10^6	1.2×10^6
19	1300	1.3×10^4	2.6×10^4	1.3×10^5	8.8×10^5	9.1×10^5
20	1200	1.2×10^4	2.4×10^4	1.2×10^5	6.8×10^5	6.9×10^5

Table 5.4: Result, no LW feedback model

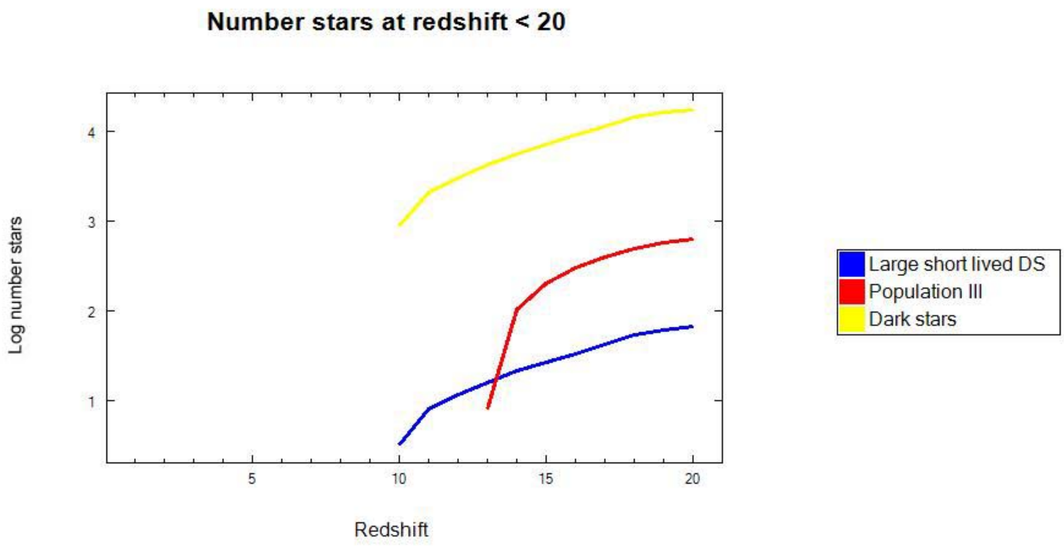

Figure 5.1: Stars in field of view below redshift 20

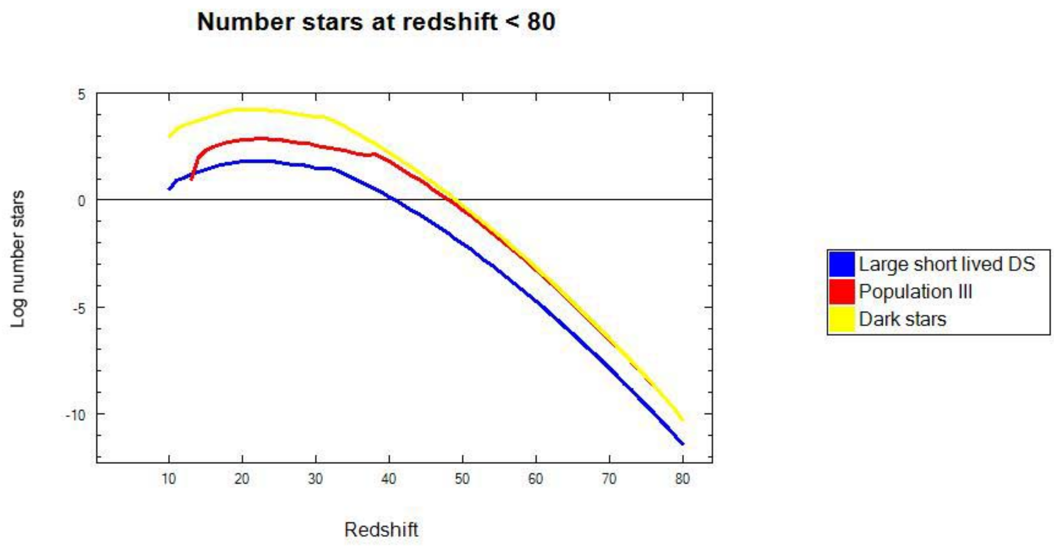

Figure 5.2: Stars in field of view below redshift 80

Chapter 6

Gravitational Lensing

Gravitational lensing is a result of Einsteins general relativity. This means that mass curves space and makes light follow curved paths through space. When light is bent around objects this can sometimes have the effect of a lens effectively magnifying and collecting more light from a smaller area behind. When the lensing object is very massive, such as a galaxy cluster, we can get magnified views of objects far away, even objects we could not possibly see by any other means. We will call the redshift of the lensing object z_l and of the magnified object, the source, z_s. The computation of gravitational lensing is often very complicated and hard to solve even with numerical methods as explained in [8]. Especially for high magnification the resulting image is often highly distorted. The lensing objects have areas of different magnification. So in rather large areas there can be a magnification of 5-10 and in smaller areas a magnification of 100 or even more. The resulting image of the source is also distorted and sometimes split up in several images, often four. From a perfectly spherical lens with the lens and source alignment also perfect a circle is the result, the radius of which is called the Einstein radius.

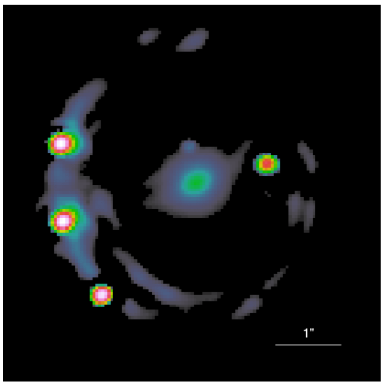

Figure 6.1: Gravitational lens RXJ1131-1231, z_l=0.295, z_s=0.658

As population III stars and dark stars are very far away, they might be impossible to observe directly. Gravitational lensing with high magnification might be a solution.

6.1 Current Observations

According to [18], the largest known Einstein radius is produced by MACS J0717.5+3745 which lies at z_l=0.546 and has a radius of 55 ± 3" for $z_s \sim 2.5$. For objects at higher redshifts it has a radius with a magnification higher than 10, which is 3.5' for $z_s \sim 8$. This might be enough to see dark stars with long lifetimes. Gravitational lensing has also been used to search for supernovas. Goobar et al.[4] have found what they claim to be a lensed supernova at $z_s \sim 0.59$ behind a galaxy in A1689. Even though found at much lower redshift than we need, this shows the feasibility of finding objects with the help of gravitational lensing that would not otherwise have been observed. Observations and theoretical work have also been done to map the matter distribution in the lens, see for example [10]. Hopefully we will find new gravitational lenses at higher redshift that could be used with JWST to probe deeper into the universe.

Chapter 7

Conclusions

The study of population III stars and dark stars represents an exciting field that is quickly evolving although still speculative. In the future, observations will be made confirming theories or forcing them to be changed or replaced. In this section I try to draw some conclusions.

Even though hardly a scientific conclusion, I think there are too many assumptions underlying dark stars for them to exist. Population III stars have to exist, dark matter has to be the right kind and behave the correct way etc. That said, there might of course be pockets where the conditions are the right ones. Anyway, because of this I will focus more on population III stars in this chapter.

7.1 Stars in the Field of View

Are we going to see any population III stars with JWST? To answer this question I calculate the apparent AB-magnitudes for the most luminous population III stars (300 $M_\odot$ according to the models used in this thesis) in the NIRCam F070W filter at different redshifts. I use the luminosity (6.59×10^6 $L_\odot$) and effective temperature (1.02×10^5 K) for a 300 $M_\odot$ population III star found in [12]. A blackbody spectrum is assumed for the stars. The results are seen in figure 7.1 with apparent magnitudes ranging between 38.1 and 39.5. For an exposure time of 100h (3.6×10^5 s) the limiting magnitude is 30.65 (see [17]), so no population III star will be observed directly according to this calculation.

In figure 7.2 the necessary magnification to observe them due to gravitational lensing is calculated for different redshifts. If the model for population III star formation assumed in this report is correct, the closest population III stars will be at redshift 13, which means a magnification of 1,000 is necessary to see it. According to table 5.2, there are only 8.1 population III stars in the field of view of JWST at redshift 13. A part of a gravitational lens with magnification higher

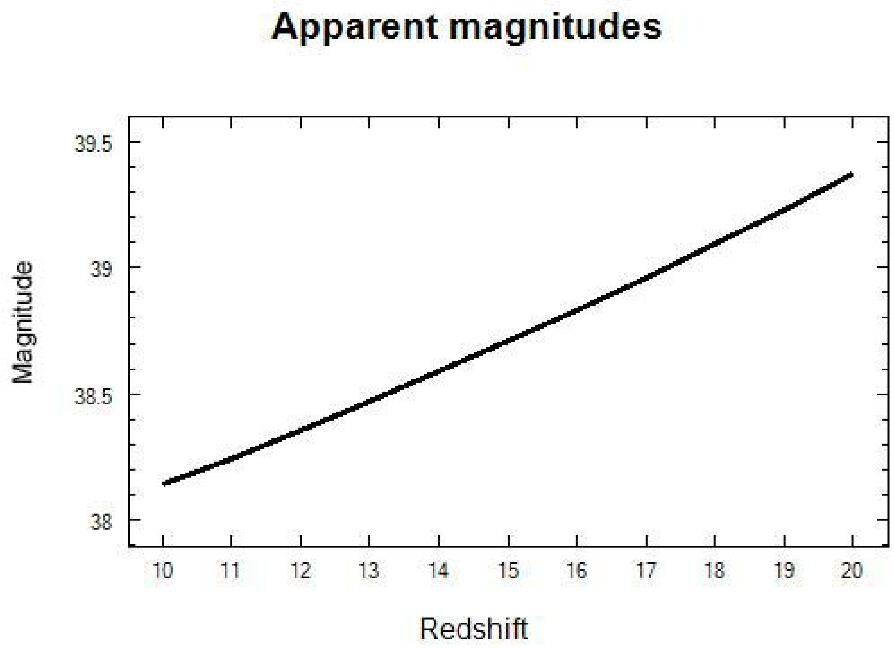

Figure 7.1: Apparent magnitude of most luminous Population III stars

than 1,000 at redshift 13 will probably have a much smaller angular size with even fewer stars in the magnified solid angle. The chance of one of them also being one of the very largest kind is very small indeed. Of course we might find gravitational lenses with a magnification of more than $\sim$ 1,000 at z=13-20 and then there will be a few thousand stars in the field of view according to table 5.2. Depending on the area of magnification, there might be a star large enough to be observed, but this is very speculative.

Probably we will see no isolated population III stars with JWST. We could of course be able to see the accumulated light of clusters of population III stars. The models in this thesis also focuses on mini halos with H_2 cooling. There might be larger $T_{vir} > 10^4$ halos forming population III stars at lower redshift. There could also be population III stars formed in pockets of unenriched gas at lower redshift.

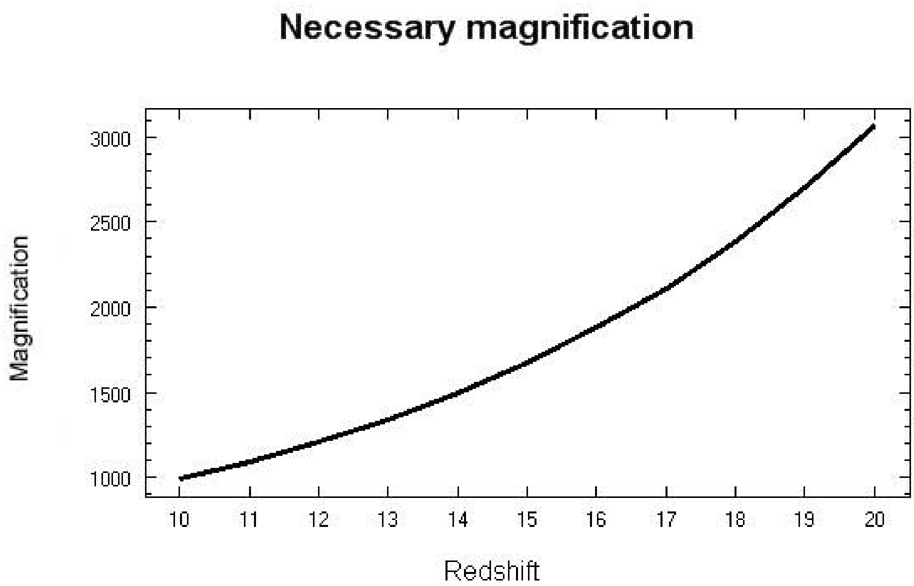

Figure 7.2: Magnification necessary to see most luminous Population III stars

Bibliography

[1] Volker Bromm, Naoki Yoshida, Lars Hernquist, and Christopher McKee. Formation of the first stars and galaxies. *arXiv*, 05 2009. [cited at p. 7]

[2] Thomas Dahlen and Claes Fransson. Rates and redshift distributions of high-z supernovae. *Astronomy and Astrophysics*, 350, 7 1999. [cited at p. 37]

[3] Sperello di Serego Alighieri, Jaron Kurk, Benedetta Ciardi, Andrea Cimatti, Emanuele Daddi, and Andrea Ferrara. The search for population iii stars. *http://arxiv.org/*, 09 2008. [cited at p. 9]

[4] A. Goobar, K Paech, V. Stanishev, R. Amanullah, T. Dahlen, J. Joensson, J.P. Kneib, C.Lidman, M. Limousin, E. Moertsell, S. Nobili, J. Richard, T. Riehm, and M. von Strauss. Near-ir search for lensed supernovae behind galaxy. *Astronomy and Astrophysics*, 2009. [cited at p. 28]

[5] F. Iocco, A. Bressan, E. Ripamonti, R. Schneider, A. Ferrara, and P. Marigo. Dark matter annihilation effects on the first star. *Monthly Notices of the Royal Astronomical Society*, 390, 06 2008. [cited at p. 1, 11]

[6] F. Iocco, A. Bressan, E. Ripamonti, R. Schneider, A. Ferrara, and P. Marigo. Effects of dark matter annihilation on the first stars. *http://arxiv.org/*, 09 2009. [cited at p. 1, 11]

[7] A. Kashlinsky. Cosmic infrared background and population iii: an overview. *http://arxiv.org/*, 10 2006. [cited at p. 10]

[8] Charles R Keeton. Computational methods for gravitational lensing. *arXiv 0102340*, 2001. [cited at p. 27]

[9] E. Komatsu, J. Dunkley, M.R. Nolta, C.L. Bennett, B. Gold, G. Hinshaw, N. Jarosik, D. Larson, M. Limon, L. Page, D.N. Spergel, M. Halpem, R.S. Hill, A. Kogut, S.S. Meyer, G.S. Tucker, J.L. Weiland, E. Wollack, and E.L. Wright. Five-year wilkinson microwave anisotropy probe observations: Cosmological interpretation. *Astrophysical Journal Suplement Series*, 180, 2009. [cited at p. 21]

[10] Masamune Oguri, Atsushi Taruya, and Yasushi Suto. Probing the core structure of dark halos with tang. *ArXiv 0105248*, 2001. [cited at p. 28]

[11] Barbara Ryden. *Introduction to Cosmology.* Pearson Addison-Wesley, 2003. [cited at p. 39]

[12] Daniel Schaerer. On the properties of massive population iii stars. *Astronomy and Astrophysics*, 11 2001. [cited at p. 23, 29]

[13] Sofia Sivertsson. Dark matter in and around stars. Licentiate Thesis, 2009. Stockholm University. [cited at p. 11]

[14] Douglas Spolyar, Peter Bodenheimer, Katherine Freese, and Paolo Gondolo. Dark stars: A new look at the first stars in the universe. *http://arxiv.org/*, 03 2009. [cited at p. 12]

[15] Michele Trenti and Massimo Stiavelli. Formation rates of population iii stars and chemical enrichment of halos during the reionization era. *The Astrophysical Journal*, 694, 03 2009. [cited at p. 7, 21, 22]

[16] Naoki Yoshida, Kazuyuki Omukai, and Lars Hernquist. Protostar formation in the early universe. *Science*, 321, 2008. [cited at p. 7]

[17] Erik Zackrisson, Pat Scott, Claes-Erik Rydberg, Fabio Iocco, Bengt Edvardsson, Göran Östlin, Sofia Sivertsson, Adi Zitrin, Tom Broadhurst, Paolo Gondolo, and Garrelt Mellema. Finding high-redshift dark stars with the james webb telescope. Submitted, 2009. [cited at p. 29]

[18] Adi Zitrin, Tom Broadhurst, Yoel Rephaeli, and Sharon Sadeh. The largest known einstein radius: Macs j0717.5+37. *Astrophysical Journal Letters*, 2009. [cited at p. 28]

Appendices

Appendix A

Comparison to Supernova rate equation

Equations similar to 5.6 are used to estimate the number of supernova detections. In this section I prove that 5.6 is equivalent to such an equation when using the same assumptions.

In [2] Dahlen and Fransson use an equation for supernova detection rate. This equation is:

$$SNR(t) = \eta \int_{t_F}^{t} SFR(t') \int_{3M_\odot}^{8M_\odot} \delta(t - t' - \Delta t_{MS} - \tau)\Phi(M) dM dt' \tag{A.1}$$

SNR(t) represents the number of supernovas produced per volume per time. I will go from this to the integral for the number of population III stars per Mpc^3 and year that is produced by using the assumptions made in this report on the supernova equation. I will assume all stars go supernova and that we will be able to sit here and count them for an entire lifetime of a population III star*.

The lifetime of the star on the main sequence is denoted Δt_{MS}. Normally this is mass dependent but since we assume a constant mass for the stars throughout this report it is a constant for us. τ in the supernova equation is the time spent as a white dwarf. This time is zero for us. Since those two values are constant and gives the lifetime of the star we can exchange them for our own lifetime τ and move the δ function outside the mass integral (since the mass dependence is gone).

$$SNR(t) = \eta \int_{t_F}^{t} SFR(t')\delta(t - t' - \tau) \int_{3M_\odot}^{8M_\odot} \Phi(M) dM dt' \tag{A.2}$$

*A rather optimistic assumption given our normal life span.

The SFR(t') is expressed in number of stars per year. We will exchange this for our own SFR but divided by M to get it in stars per year. The limits on the mass integral in the supernova formula are set to include the stars that go supernova in a special way. Since we assume all the stars go supernova this integral will evaluate to 1. The η gives the fraction of those stars that explode as a result of binary accretion. Since we assume all stars go off as supernova this value will also be 1. We are left with:

$$SNR(t) = \int_{t_F}^{t} SFR(t')/M\delta(t - t' - \tau)dt' \tag{A.3}$$

This integral over a δ function evaluates to:

$$SNR(t) = SFR(t - \tau)/M \tag{A.4}$$

And it seems logical that the stars formed one star life time ago should go supernova at a time one life time later. If we assume that we sit for an entire life time of a star and count the supernovas from this volume element we get the number:

$$\int_{t}^{t+\tau} SNR(t)dt = \int_{t}^{t+\tau} SFR(t - \tau)/Mdt = \int_{t-\tau}^{t} SFR(t)/Mdt \tag{A.5}$$

This we recognize as the equation 5.2. So by counting supernovas we get the same number of stars per Mpc^3 at a cosmic time. The rest of the derivation of equation 5.6 is really just a calculation of volume with the correct number of stars per Mpc^3 at the correct cosmic time time inserted so it is the same in the supernova case.

Appendix B

Cosmic Distances

Normally when speaking about distances in our approximately euclidean space there is only one unique distance. In cosmology we use several different distances with different interpretations.

In the reasoning below I keep to a flat expanding universe of the type we seem to be living in, see [11].

B.1 Proper distance

We observe objects at certain redshifts which corresponds to a certain time and distance. If we assume that this observed object "floats" with the expansion of the universe until it is at the same time after the big bang as we are then the distance to it is the proper distance. If we could stop the universe expansion and measure the distance to the object we would get the proper distance. In a sense this is the "real" distance.

B.2 Angular Size Distance

When observing a large object it spans a certain angle in the sky. This angle depends on the objects size and its distance. In an expanding universe this distance is a special entity which has to be calculated. It turns out that the angular distance is equal to the proper distance at the time the light was emitted from the object in a flat universe. In this sense one can say that all light we see in the universe follow the path of the angular size distance when viewed as a function of time. This is so since all light from earlier times has to be at the same proper distance as new light emitted since light speed is constant. Typically the angular size distance goes towards zero when approaching the Big Bang.

Since this reasoning is only valid in a flat universe it is harder to find an interpretation of the angular size distance in other universes. But since we live in a flat universe (probably) it is a usable interpretation.

B.3 Luminosity Distance

When the universe is expanding the light from a source decreases both because of the distance it was emitted from (angular size distance) and because the light loses energy because of the expansion. The expansion also causes the photons to increase their spatial distances. This give the impression that objects are very far away when measuring the flux from them. When measuring their flux and comparing to their intrinsic luminosity a "distance" can be inferred *.

B.4 Hubble Distance

The Hubble distance at each point in time corresponds to the proper distance at which objects are receding faster than light. In the early Universe the Hubble distance is shorter than the angular size distance. This means that those objects actually receded faster than light when their light was emitted. This can be since the light when approaching us enters space that recedes slower and slower. Finally it recedes slower than light. This also means that the angular size distance reaches its maximum when crossing the Hubble distance as can be seen in B.1. At this point the light has the same speed as the expansion of the universe.

B.5 Horizon Distance

The horizon distance is the maximum proper distance of any object we can see. This distance is zero at Big Bang and then grows over time. The path through the universe that currently has the horizon distance has a higher proper distance at each point in time than the horizon distance at that time.

B.6 Observing at High Redshift

These distances set the stage for our universe and the stars we try to observe. In figure B.1 the evolution of the universe from the Big Bang until now are seen as a function of time. The marks over the graph shows at what redshift an object at that particular cosmic time is observed. The black line marks an object at redshift infinity, that is the farthest object we can see and of course its proper distance now is the current horizon distance. The purple and green lines are stars

*Since it is hard to find a real interpretation for this distance I think it should really be called a luminosity factor or something similar instead of a luminosity distance.

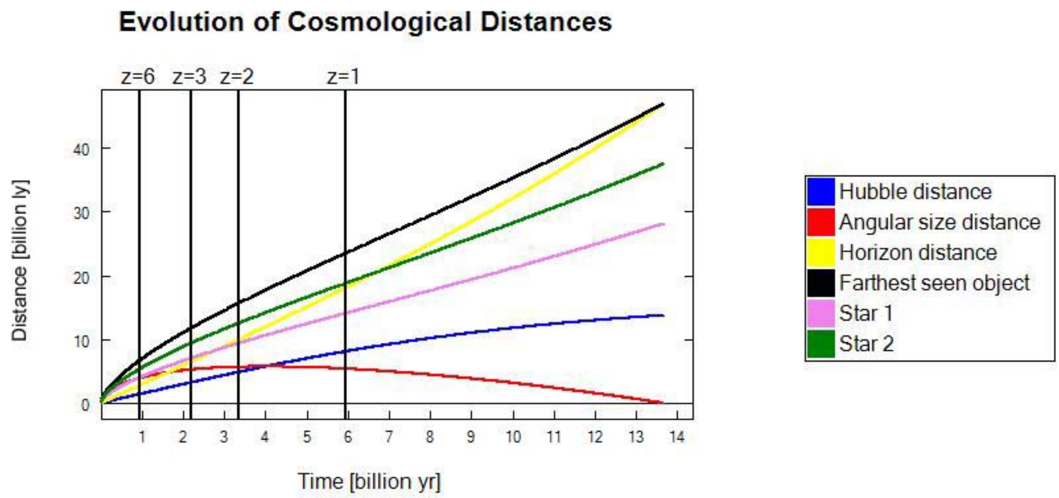

Figure B.1: Expansion of the universe

that we potentially could detect. Their proper distance follow the scale factor of course and crosses the horizon distance at 3 and 6.7 billion years respectively meaning that at those particular times these stars had the role of the farthest object viewable having infinite redshift. They are both farther away than the Hubble distance, meaning that they always have been receding from us faster than light.

Looking at figure B.2 we can see at what redshift we will observe these stars. This is where there life lines (the purple and green lines crosses the angular size distance (since all the light we see follows this path). Reading off the top of the chart the redshifts are approximately 6.5 and 25 respectively. So the green and purple stars are formed and live along their life lines until they cross the angular size distance where they emit the light we see. If we wait the angular size distance curve will move upwards in the graphs and consequently will cross the stars life lines later and we will see them grow older.

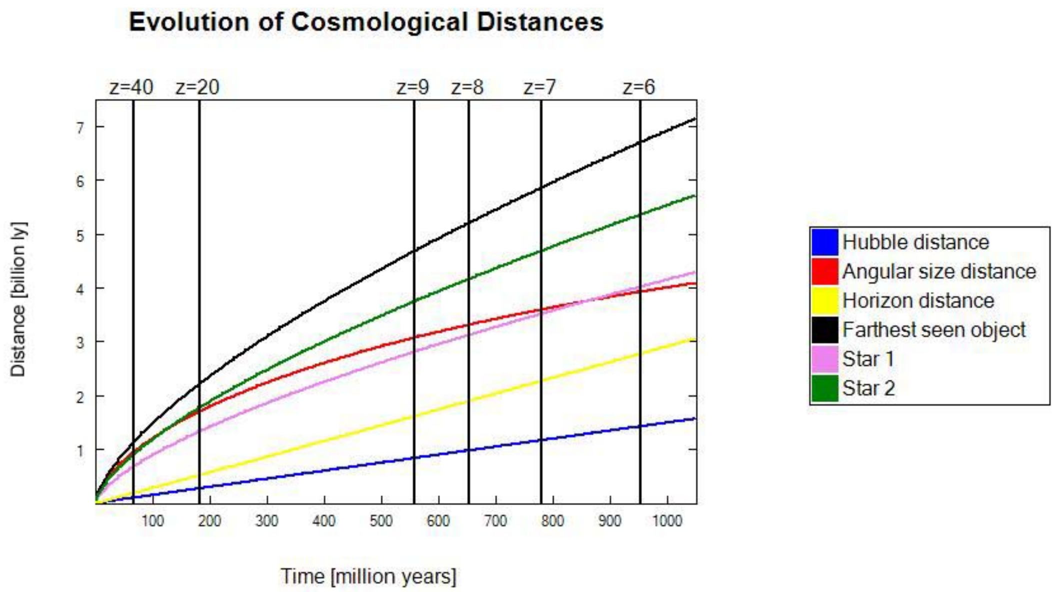

Figure B.2: Expansion of the universe, first billion years

Appendix C

Code

In this appendix I show the code mainly used for calculations in the thesis. It is code that calculate the number of stars in the field of view of JWST.

This appendix contains a printout of the class, ObservableStars, most used in this thesis. There is also a small explanation of classes used by this class in C.1. When a code line has too many characters to fit on a printout line part has been moved to the next line and been indented 8 character spaces.

C.1 Support Classes

The ObservableStars class uses and depends on several other classes. Here is a small list with explanations of those:

AngleMeasurement Handles measurement of angles and conversions between different ways of measuring angles.

ApplicationAstronomy Static class for calculating and managing astronomy related objects that can be easily accessed by the entire application. In the ObservableStars class the concordance universe is accessed.

ArraySummation.MidPointSum Sums a real valued function over an array of x-values. In each bin formed by the x-values the mid point value is evaluated and multiplied with the width of the bin. All bins are then summed.

Conversion Static class containing different conversion factors and other static classes containing conversion factors. For example years to seconds.

DiscreteBasedFunction Class that takes two arrays X and Y of equal length. The class then linearly interpolates a y value when inserting an x value with the help of those arrays.

Math Static class containing mathematical functions and constants.

PhysicalConstant Static class containing different physical constants. For example the speed of light.

StarFormationRateDataSet Handles the connection to the database where the star formation data is stored. Loads the data and returns it to the program as arrays.

StarFormationRateDataSet.StarFormationRateDataInfo Struct of arrays containing the data for a certain SFR model which is returned by the StarFormationRateDataSet class.

C.2 Observable Star Class

```
/// <summary>
/// Class for calculating how many stars will be in the field of view of JWST
/// </summary>
public class ObservableStars
{

#region Private/protected members

protected StarFormationRateDataSet.StarFormationRateDataInfo _model1starformationratedata;
protected StarFormationRateDataSet.StarFormationRateDataInfo _model2starformationratedata;
protected StarFormationRateDataSet.StarFormationRateDataInfo _model3starformationratedata;
protected DiscreteBasedFunction _model1timetoformationrate;
protected DiscreteBasedFunction _model2timetoformationrate;
protected DiscreteBasedFunction _model3timetoformationrate;
protected StarFormationRate _starformationratemodel;
protected DiscreteBasedFunction _timetoformationrate;
protected DiscreteBasedFunction _timetojameswebbarea;
protected DiscreteBasedFunction _redshifttojameswebbarea;
protected double _starlifetime;
protected double _starmass;

#endregion

#region Constructors

/// <summary>
/// Initializes basic values and calculates concordance universe, James Webb area and star
/// formation rate
/// </summary>
public ObservableStars()
{
    ApplicationAstronomy.CalculateConcordanceUniverse();
    CalculateJamesWebbarea();
    CalculateStarFormationRate();
}

#endregion
```

```
#region Public methods

/// <summary>
/// Sums number of stars for given mass, life time and SFR model in a redshift interval
/// </summary>
/// <param name="numbersteps"></param>
/// <param name="Zlow"></param>
/// <param name="Zhigh"></param>
/// <returns></returns>
public double NumberStarsInRedshiftIntervalJWST(int numbersteps, double Zlow, double Zhigh)
{
    return ArraySummation.MidPointSum(StarsAtRedshiftPerDeltaDistance, Zlow, Zhigh, numbersteps);
}

#endregion

#region Private/protected methods

/// <summary>
/// Calculates star formation per year per Mpc^3
/// </summary>
protected void CalculateStarFormationRate()
{
    CalculateStarFormationRate(ref _model1starformationratedata, ref _model1timetoformationrate,
            StarFormationRate.Basic);
    CalculateStarFormationRate(ref _model2starformationratedata, ref _model2timetoformationrate,
            StarFormationRate.ReducedEscapeFraction);
    CalculateStarFormationRate(ref _model3starformationratedata, ref _model3timetoformationrate,
            StarFormationRate.NoLymanWernerFeedback);
}

/// <summary>
/// Calculates star formation per year per Mpc^3 for one SFR model
/// </summary>
/// <param name="sfrdataset"></param>
/// <param name="timetoformationrate"></param>
/// <param name="starformationratemodel"></param>
protected void CalculateStarFormationRate(ref StarFormationRateDataSet.StarFormationRateDataInfo sfrdataset,
        ref DiscreteBasedFunction timetoformationrate, StarFormationRate starformationratemodel)
{
    sfrdataset = StarFormationRateDataSet.Set.GetStarFormationRateData((int)starformationratemodel);
    DiscreteBasedFunction redshifttoformationrate = new DiscreteBasedFunction(sfrdataset.Redshift,
            sfrdataset.PopIIIH2, false);
    double[] formationrate = new double[ApplicationAstronomy.ConcordanceUniverse.PastTimeUniverse.Length];

    for (int i = 0; i < ApplicationAstronomy.ConcordanceUniverse.PastTimeUniverse.Length; i++)
    {
        double redshift = ApplicationAstronomy.ConcordanceUniverse.PastTimeUniverse.TimeToRedshift.Y[i];
        if (redshift < redshifttoformationrate.LowerBound || redshift > redshifttoformationrate.UpperBound)
            formationrate[i] = 0;
        else
            formationrate[i] = redshifttoformationrate.Calculate(redshift) / Conversion.Year.GetConversionToSIfactor();
    }
    timetoformationrate = new DiscreteBasedFunction(
            ApplicationAstronomy.ConcordanceUniverse.PastTimeUniverse.TimeToScaleFactor.X, formationrate, false);
}
```

```
/// <summary>
/// Method to be integrated for recieving number of stars
/// </summary>
/// <param name="Z"></param>
/// <returns></returns>
protected double StarsAtRedshiftPerDeltaDistance(double Z)
{
    double starspermegaparsec = StarsPerCubedMeter(
            ApplicationAstronomy.ConcordanceUniverse.RedshiftUniverse.RedshiftToTime.Calculate(Z));
    double area = _timetojameswebbarea.Calculate(
            ApplicationAstronomy.ConcordanceUniverse.RedshiftUniverse.RedshiftToTime.Calculate(Z));

    DiscreteBasedFunction redshifttotimederivative = DiscreteBasedFunction.CalculateDerivative(
            ApplicationAstronomy.ConcordanceUniverse.RedshiftUniverse.RedshiftToTime);
    double c = PhysicalConstant.SpeedOfLight.PhysicalValue.Value;
    return -area * starspermegaparsec * c * redshifttotimederivative.Calculate(Z) * Math.Pow(1 + Z, 3);
}

/// <summary>
/// Calculates stars per cubed meter
/// </summary>
/// <param name="t"></param>
/// <returns></returns>
protected double StarsPerCubedMeter(double t)
{
    double starttime = Math.Max(t - _starlifetime, _timetoformationrate.LowerBound);
    double endtime = Math.Min(t, _timetoformationrate.UpperBound);
    double solarmassesformed = 0;
    if (endtime > starttime)
        solarmassesformed = ArraySummation.MidPointSum(_timetoformationrate.X, _timetoformationrate.Y, starttime, endtime);
    double conversiontometer = Conversion.Astronomy.Distance.Parsec.Copy(3, PowerOfTen.mega).GetConversionToSIfactor();
    return solarmassesformed / (conversiontometer * _starmass);
}

/// <summary>
/// Calculates James Webb observed area as functions of time and redshift
/// </summary>
protected void CalculateJamesWebbarea()
{
    AngleMeasurement angle = new AngleMeasurement(0, 2.2, 0);
    double angulararea = Math.Pow(angle.Radians, 2);
    double[] jameswebbareapertime = new double[ApplicationAstronomy.ConcordanceUniverse.PastTimeUniverse.Length];
    for (int i = 0; i < jameswebbareapertime.Length; i++)
        jameswebbareapertime[i] = angulararea * Math.Pow(
                ApplicationAstronomy.ConcordanceUniverse.PastTimeUniverse.TimeToAngularDistance.Y[i], 2);
    _timetojameswebbarea = new DiscreteBasedFunction(
            ApplicationAstronomy.ConcordanceUniverse.PastTimeUniverse.TimeToAngularDistance.X, jameswebbareapertime, false);

    double[] jameswebbareaperredshift = new double[ApplicationAstronomy.ConcordanceUniverse.RedshiftUniverse.Length];
    for (int i = 0; i < jameswebbareaperredshift.Length; i++)
        jameswebbareaperredshift[i] = angulararea * Math.Pow(
                ApplicationAstronomy.ConcordanceUniverse.RedshiftUniverse.RedshiftToAngularDistance.Y[i], 2);
    _redshifttojameswebbarea = new DiscreteBasedFunction(
            ApplicationAstronomy.ConcordanceUniverse.RedshiftUniverse.RedshiftToAngularDistance.X, jameswebbareaperredshift, false);
}

#endregion
```

```
#region Public enum

/// <summary>
/// Enum for tracking what SFR model the class is working with
/// </summary>
public enum StarFormationRate
{
    Basic = 1,
    ReducedEscapeFraction = 2,
    NoLymanWernerFeedback = 3
}

#endregion

#region Properties

/// <summary>
/// Returns or sets what SFR model the class is working with, if set, a pointer for
/// a time to formation rate is set to the correct function
/// </summary>
public StarFormationRate StarFormationRateModel
{
    get
    {
        return _starformationratemodel;
    }
    set
    {
        _starformationratemodel = value;
        if (_starformationratemodel == StarFormationRate.Basic)
            _timetoformationrate = _model1timetoformationrate;
        else if (_starformationratemodel == StarFormationRate.ReducedEscapeFraction)
            _timetoformationrate = _model2timetoformationrate;
        else if (_starformationratemodel == StarFormationRate.NoLymanWernerFeedback)
            _timetoformationrate = _model3timetoformationrate;
    }
}

/// <summary>
/// Returns model 1 SFR data
/// </summary>
public StarFormationRateDataSet.StarFormationRateDataInfo Model1StarFormationRateData
{
    get
    {
        return _model1starformationratedata;
    }
}

/// <summary>
/// Returns model 2 SFR data
/// </summary>
public StarFormationRateDataSet.StarFormationRateDataInfo Model2StarFormationRateData
{
    get
    {
        return _model2starformationratedata;
    }
}

/// <summary>
/// Returns model 3 SFR data
/// </summary>
public StarFormationRateDataSet.StarFormationRateDataInfo Model3StarFormationRateData
{
    get
    {
        return _model3starformationratedata;
    }
}
```

```
/// <summary>
/// Returns or sets mass of star in solar masses
/// </summary>
public double StarMass
{
    get
    {
        return _starmass;
    }
    set
    {
        _starmass = value;
    }
}

/// <summary>
/// Returns or sets life time of star in millions of years
/// </summary>
public double StarLifeTime
{
    get
    {
        return _starlifetime;
    }
    set
    {
        _starlifetime = value;
    }
}

#endregion

}
```

List of Symbols and Abbreviations

Abbreviation	Description	Reference
ACS	Attitude Control System	4.4.4
CCD	Charge Coupled Device	4.4.2
CIB	Cosmic Infrared Background	2.3
CMB	Cosmic Microwave Background	1.1.3; 2
CSA	Canadian Space Agency	4
ESA	European Space Agency	4
FGS	Fine Guidance Sensor	4.4.4
JWST	James Webb Telescope	4; 4.3; 4.4; 5; 6.1; 7.1; 7.1; C
$L_\odot$	1 solar luminosity	7.1
LW	Lyman-Werner	2.2; 2.2.1; 2.2.2; 2.2.3
$M_\odot$	1 solar mass	2.1; 2.2.1; 5.1; 7.1
MIRI	Mid-Infrared Instrument	4.4.1
NASA	National Space Agency	4
NIRCam	Near-Infrared Camera	4.4.2; 7.1
NIRSpec	Near-Infrared Spectrograph	4.4.3
SFR	Star Formation Rate	5.3; A; C.1
SNR	Supernova rate	A
UV	Ultra Violet	2.1
WIMP	Weakly Interacting Massive Particle	3.1

List of Figures

List of Tables

Index